

Hall conductivity of Sierpinski carpet

Askar A. Iliasov,^{1,2,*} Mikhail I. Katsnelson,¹ and Shengjun Yuan^{2,1,†}

¹*Institute for Molecules and Materials, Radboud University,
Heyendaalseweg 135, 6525AJ Nijmegen, The Netherlands*

²*Key Laboratory of Artificial Micro- and Nano-structures of Ministry of Education
and School of Physics and Technology, Wuhan University, Wuhan, China*

(Dated: May 5, 2022)

We calculate the Hall conductivity of Sierpinski carpet using Kubo-Bastin formula. The quantization of Hall conductivity disappears when we go further and further from the square sample without holes to the fractal structure. The Hall conductivity is no more proportional to the Chern numbers. Nevertheless, these quantities behave in a similar way showing some reminiscence of a topological nature of the Hall conductivity. We also study numerically bulk-edge correspondence and find that the edge states become less manifested with increasing the depth of Sierpinski carpet.

INTRODUCTION

Fractals were very popular in 1980th and various properties of fractals were intensively studied that time [1–3]. Most of these works were focused on classical fractal systems; at the same time, it turned out that their quantum properties are also unusual and interesting. For example, fractals have Cantor-like energy spectrum, which make them similar to quasicrystals [4]. In that time, studies of quantum properties of fractal structures was of purely fundamental interest. Recent progress in technologies can produce fractals by both nanofabrication methods and manipulations with individual molecules on metal surfaces [5–8]. This creates a boost to new researches in the field. Recent theoretical works concerning quantum effects in fractals consider transport properties [9–11], plasmons [12], Anderson localization [13, 14], topological properties [15, 16] and other related topics [17–20].

It was established in the seminal work [21] that the off-diagonal (Hall) conductivity of two-dimensional electron gas in magnetic field is proportional to the so called Chern number and therefore is closely related to topological properties of the system. This relation is based on translational invariance of the system, and it is unclear what will be the situation in quasiperiodic or fractal structures where the translational invariance is absent. There are works about quantum Hall effect concerning quasicrystals in different dimensions and they reveal non-trivial topological properties [22–24] as well as disordered systems [25, 26], but the researches about fractals are scarce. Therefore it is natural to investigate conductivity of fractals due to possible experimental applications. Apart from possible relevance for experiments with novel fractal structures, the clarification of this issue can provide better understanding of fracton topological order [27, 28].

It is known for systems with integer dimensions that quantization of Hall conductivity is closely related with existence of edge states [29–31]. The notions of edge and bulk can be well defined for systems without holes, or

at least for a system, which has integer dimension and finite number of holes. Fractals have infinite number of holes, and these holes are dense. Therefore the difference between edge state and bulk state should be carefully checked. This can be useful for better understanding of Hall conductivity of fractals. One way to do this is to study various of approximations to a fractal with holes on different scales.

Chern numbers for Sierpinski carpet were calculated in Ref. 15. The authors have concluded that Chern numbers are no more integer everywhere but are still quantized in some energy ranges; in this sense, the fractal still possess non-trivial topological properties. However, it is not obvious if behaviour of Hall conductivity will be the same for Sierpinski carpet.

In order to answer that question, in this work we calculate the Hall conductivity and quasi-eigenstates for various iterations of Sierpinski carpet and investigate how they behave under increasing of depth of fractal. We also compare our results with the calculated Chern numbers from the article [15].

THE MODEL

To study the fractal structures, we use the single-orbital tight-binding Hamiltonian in the nearest-neighbor approximation, that is, the same model as in Refs. 9 and 10:

$$H = -t \sum_{\langle ij \rangle} e^{i\phi_{ij}} c_i^\dagger c_j, \quad (1)$$

where c_i^\dagger creates fermion on a lattice site i , and $\langle ij \rangle$ denotes the nearest-neighbor sites belonging to the studied fractal. The influence of magnetic field is modeled by the standard Peierls substitution: $\phi_{ij} = 2\pi/\Phi_0 \int_i^j \mathbf{A} \cdot d\mathbf{r}$, where \mathbf{A} is the vector potential and $\Phi_0 = hc/e$ is the flux quantum. We use Landau gauge $\mathbf{A} = (-By, 0, 0)$.

We start with the square lattice of the size $3^{D_f} \times 3^{D_f}$. Then, we iteratively delete holes, which give us the realizations of Sierpinski carpet with different depth. At

first, we delete central hole of the size $3^{D_f-1} \times 3^{D_f-1}$, then we delete holes with the size $3^{D_f-2} \times 3^{D_f-2}$, and so on. We can stop at any number of iterations I_f less than D_f . The maximum depth of fractal on a given lattice is D_f , in this case the size of a hole is equal to one site. The examples of different iterations are given in Fig. 1

These structures with two parameters I_f and D_f describe various approximations of Sierpinski carpet as well as transition from usual square lattice with dimension 2, to lattice with fractional dimension equal to $\ln 8 / \ln 3$ for Sierpinski carpet.

In order to calculate density of states and Hall conductivity we use the approaches described in Refs. 32 and 33, and 34 and 35, respectively. Using this method, we are able to calculate physical properties for 6 iterations of Sierpinski carpet.

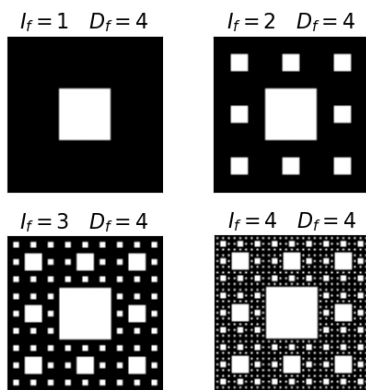


FIG. 1. The examples of studied fractal structures. The size of the large square is $3^{D_f} \times 3^{D_f}$ sites with $D_f = 4$ and different number of iterations I_f . With every iterations, new holes are deleted. The size of smallest holes is $3^{D_f-I_f} \times 3^{D_f-I_f}$.

RESULTS

Density of states

Let us at first shortly describe the numerical method. We calculate density of states (DoS) for different fractal depth and iterations using method based on the time evolution operator [32, 33]. We start the evolution of a quantum system with a random initial state $|\psi\rangle$, which is normalized so that $|\psi|^2 = 1$. The density of states is calculated via Fourier transform of the correlation function and averaging over initial random samplings [32, 33]:

$$\begin{aligned} d(\epsilon) &= \langle \psi | \delta(\epsilon - H) | \psi \rangle = \\ &= \frac{1}{2\pi} \int_{-\infty}^{+\infty} e^{i\epsilon\tau} \langle \psi | e^{-i\tau H} | \psi \rangle d\tau \end{aligned}$$

Since the density of states is a self-averaged quantity, it does not depend on the choice of the state $|\psi\rangle$ for large enough systems.

In Fig. 2, we show the calculated density of states for various magnetic fields corresponding to Φ/Φ_0 changing from 0 to 0.5, Φ is the magnetic flux through the smallest element for a given structure. The energy E there and further in all cases is measured in values of hoppings t of the Hamiltonian (1). These pictures of Hofstadter butterflies [36] are calculated for $D_f = 6$ and $I_f = 0, 2, 4, 5$. The figure demonstrates fractal structure of states and gaps due to additional frequency in hoppings associated with magnetic flux.

From these pictures one can see that for $I_f = 0, 1, 2, 4$ DoS is basically the same for all magnetic fields. The structure of Hofstadter butterfly with $I_f = 5$ is different from the previous cases, there are a lot of additional states and small gaps open for some magnetic fields. Therefore, $I_f = 5$ seems to be the minimal depth which is needed to catch the peculiarities of quantum states in this particular fractal.

In Fig. 3, DoS is displayed for the fractal with $I_f = D_f = 6$ and $\Phi/\Phi_0 = 0.25$. The change from I_5 to I_6 is clear: the gap opens in the middle of the spectrum, and there are more states between peaks (around energy $E = 2$). In comparison with this figure, the density of states for $I_f = 5$ is flattened in that region.

We also calculated DoS for $I_f = D_f = 4$ and $I_f = D_f = 5$. The results visually almost indistinguishable from the case $I_f = D_f = 6$. Therefore the DoS converges for samples with maximum number of iterations and approach the thermodynamic limit of a full fractal. For cases with $I_f < D_f < 6$ we also observe that DoS changes little while $I_f < D_f - 1$ and at $I_f = D_f - 1$ there is transition to another regime. Due to this transition, one cannot properly approximate the full fractal, if the smallest holes are absent in the sample.

The occurrence of the transition can be explained by the following reasoning. Before transition point there is still well defined bulk and effective dimension of a sample is integer. The holes in a sample can be seen as some additional disorder. When I_f becomes equal to 5 the distance between holes becomes comparable to the size of a site. Only at this point, the effective dimension of a sample becomes non-integer. The difference between cases $I_f = 5$ and $I_f = 6$ also can be explained by difference in their non-integer dimensions. The proper approximation of Sierpinski carpet is only if $I_f = D_f$.

We can think about this effect as a crucial property of exact scaling symmetry of fractals. So that even the smallest breaking of scaling symmetry leads to effective integer dimension, not fractional. Every site is an edge site in a sample with maximum fractal depth. This condition strongly restricts geometry of paths in a sample. We can assume therefore that the scaled geometry plays a decisive role in the properties of a fractal and it is closely

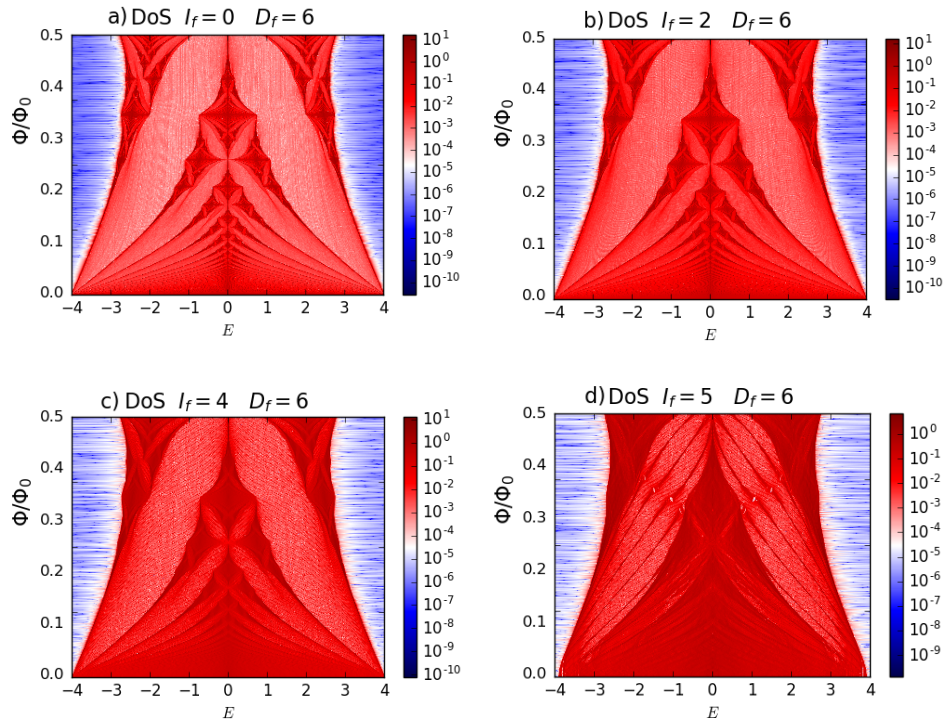


FIG. 2. Pictures of DoS depending of magnetic field – Hofstadter butterflies (magnetic field B corresponds to variations of Φ/Φ_0 from 0 to 0.5) for different iterations for Sierpinski carpet in a square of the size $3^{D_f} \times 3^{D_f}$ and $D_f = 6$ a) is $I_f = 0$ iteration, b) is $I_f = 2$ iterations, c) is $I_f = 4$ iterations, d) is $I_f = 5$ iterations. The differences between a), b) and c) are small. New peaks and gaps appear in the picture d).

connected to the space of paths in Sierpinski carpet.

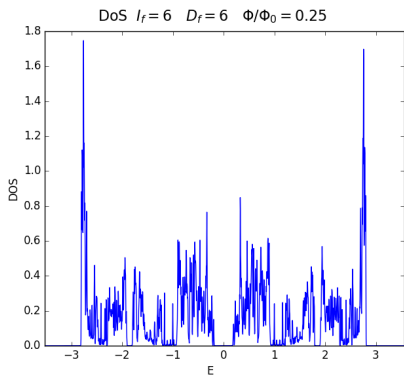


FIG. 3. The density of states for Sierpinski carpet with $D_f = I_f = 6$, maximum number of iterations for the square with size $3^{D_f} \times 3^{D_f}$, $\Phi/\Phi_0 = 0.25$. In comparison with Fig. 2 d), a gap appears in the middle of the spectrum.

Hall conductivity

In order to calculate the Hall conductivity, we use the approach from Ref. 34 and 35. The method is based on

the so called Kubo-Bastin formula:

$$\sigma_{\alpha\beta} = \frac{i\hbar e^2}{A} \int_{-\infty}^{+\infty} d\epsilon f(\epsilon) \text{Tr} \langle v_\alpha \delta(\epsilon - H) v_\beta \frac{dG^+(\epsilon)}{d\epsilon} - v_\alpha \delta(\epsilon - H) v_\beta \frac{dG^-(\epsilon)}{d\epsilon} \rangle$$

where A is the area of the sample, $f(\epsilon) = \frac{1}{\exp(\epsilon - \mu)/T}$ is the Fermi-Dirac distribution, T is temperature, μ is the chemical potential, v_α is α component of velocity operator, $G^\pm = 1/(\epsilon - H \pm i\eta)$ are the Green's functions. In this formula we also use averaging over random samplings as we did for the density of states. We can expand Green's functions and delta function on Chebyshev polynomials and then for conductivity we obtain:

$$\sigma_{\alpha\beta} = \frac{4\hbar e^2}{\pi A} \frac{4}{\Delta E^2} \int_{-1}^1 d\tilde{\epsilon} \frac{f(\tilde{\epsilon})}{(1 - \tilde{\epsilon}^2)^2} \sum_{m,n} \Gamma_{nm}(\tilde{\epsilon}) \mu_{m,n}^{\alpha\beta}(H) \quad (2)$$

where $\tilde{\epsilon}$ is rescaled energy within $[-1, 1]$, ΔE is the energy range of spectrum, $\mu_{m,n}^{\alpha\beta}(H)$ and $\Gamma_{nm}(\tilde{\epsilon})$ are described by the following formulas:

$$\Gamma_{nm}(\tilde{\epsilon}) = T_m(\tilde{\epsilon})(\tilde{\epsilon} - in\sqrt{1 - \tilde{\epsilon}^2}e^{in \arccos(\tilde{\epsilon})}) \\ + T_n(\tilde{\epsilon})(\tilde{\epsilon} + im\sqrt{1 - \tilde{\epsilon}^2}e^{-im \arccos(\tilde{\epsilon})})$$

and

$$\mu_{m,n}^{\alpha\beta}(H) = \frac{g_m g_n}{(1 + \delta_{n0})(1 + \delta_m)}$$

We use Jackson kernel g_m to smooth Gibbs oscillations due to truncation of the expansion in Eq. (2) [34].

Our results for σ_{xy} are shown in Fig. 4. The Hall conductivity was calculated for $\Phi/\Phi_0 = 0.25$, $D_f = 6$ and $I_f = 0, 4, 5, 6$.

The Hall conductivity behaves similarly to the DoS pictures. The differences between $I_f = 0$ and $I_f = 4$ are quite small, although there are fluctuations in the case of $I_f = 4$. The structure is similar, there are plateaus, which correspond to relatively small values of DoS, in the middle of spectrum and between peaks. These plateaus are indication of relation of Hall conductivity to topological invariants. One can see clear transition at $I_f = 5$ iterations. The plateau in the middle of spectrum is smeared at $I_f = 5$ and fluctuations become much stronger.

The picture of Hall conductivity for $I_f = D_f = 6$ demonstrates a completely different behaviour. We can compare these results to Chern numbers calculated in Ref. 15 for $I_f = D_f = 4$. In general, Hall conductivity looks similar to the Chern number, however, there are more fluctuations and peaks that are absent in the behaviour of Chern numbers.

There are two regions which correspond to quantized Chern number, around $E = \pm 1$. These regions occur after smearing of peaks in less iteration depths I_f . From the previous plateaus there remain only small parts around $E = \pm 2.5$ and a part of region around $E = \pm 1$, these regions correspond to almost quantized Chern number. It is interesting that regions around $E = \pm 1$ with quantized Chern numbers are not flat plateaus. This was checked for different numbers of random samples and fluctuations were stable. The central gap in DoS corresponds to conductivity $\sigma_{xy} = 0$, as well as the Chern number, which is equal to 0.

We also added disorder to the sample by deleting random sites. The results are shown in Fig. 5, where we deleted around 20% of sites in the sample. We see that DoS as well as Hall conductivity are stable with respect to the disorder. Moreover, one can see even less fluctuations on the pictures in comparison with Fig. 4. Thus, we can conclude that fractals are stable to disorder as well as systems with integer dimensions.

Particularly this result could be expected, since holes in a fractal sample already could be seen as a kind of disorder. Therefore additional disorder should not effect on physical properties unless this disorder is large enough.

However, there are subtleties since exact scaling symmetry on all scales is important for correct approximation of the fractal.

Quasi-eigenstates

It is known that the edge states in quantum Hall systems are closely related to their topological properties [29, 30, 37]. Occurrence of the edge states corresponds to quantized Chern numbers (bulk-edge correspondence). Therefore it is naturally to assume that transitions with increasing I_f in DoS and Hall conductivity will be seen in the edge states as well. To explore this question we calculated quasi-eigenstates for Sierpinski carpet. Quasi-eigenstates and probability current were calculated by the same method of averaging [33]. For the probability current, we use the formula [38]:

$$\mathbf{j} = \text{Re}(\psi^* \mathbf{v} \psi) = \frac{\hbar}{m_e} \text{Im}(\psi^* \nabla \psi) - \frac{q}{m_e} \mathbf{A} |\psi|^2 \quad (3)$$

At first let us take a look to states corresponding to plateaus and peaks for some iterations with enough number of holes, but with regular behaviour of Hall conductivity. For more readable pictures we used samples with size $D_f = 5$. Examples of bulk and edge states for $I_f = 3$ iterations are shown in Fig. 6. Edge states, which are shown on the left side of picture, correspond to energies $E = 1.51$ and $E = 2.59$. Bulk states, which are shown on the right side of picture, correspond to energies $E = 1.09$ and $E = 2.83$. Edge states correspond to plateaus in Hall conductivity and bulk states correspond to slopes of peaks. We see that edge states can be localized along holes on different scales i.e. only the central hole, central hole and holes of second iterations and so on.

Examples of bulk and edge states for $I_f = 5$ iterations (i.e. fractal with maximum depth) are shown in Fig. 7. Edge states, which are shown on the left side of picture, correspond to energies $E = 1.33$ and $E = 2.59$. Bulk states, which are shown on the right side of picture, correspond to energies $E = 1.57$ and $E = 2.83$. Edge states correspond to quantized and almost quantized Chern number. There is a reminiscence of this quantization in Hall conductivity.

We see that edge states in a full fractal differ from edge states in Fig. 6. In a sample with $I_f = 3$ iterations, current is localized along borders in a homogeneous pattern, there are just lines of currents along edges. However, in a full fractal, current has more complex pattern, for example, it can be localized along small holes, which are close to an edge. This deformation of edge current can be a reason of absence of plateaus in Hall conductivity even for regions with quantized Chern number. We also see that bulk states in a sample with $I_f = 5$ iterations demonstrate more symmetric behaviour. This is, obviously, the

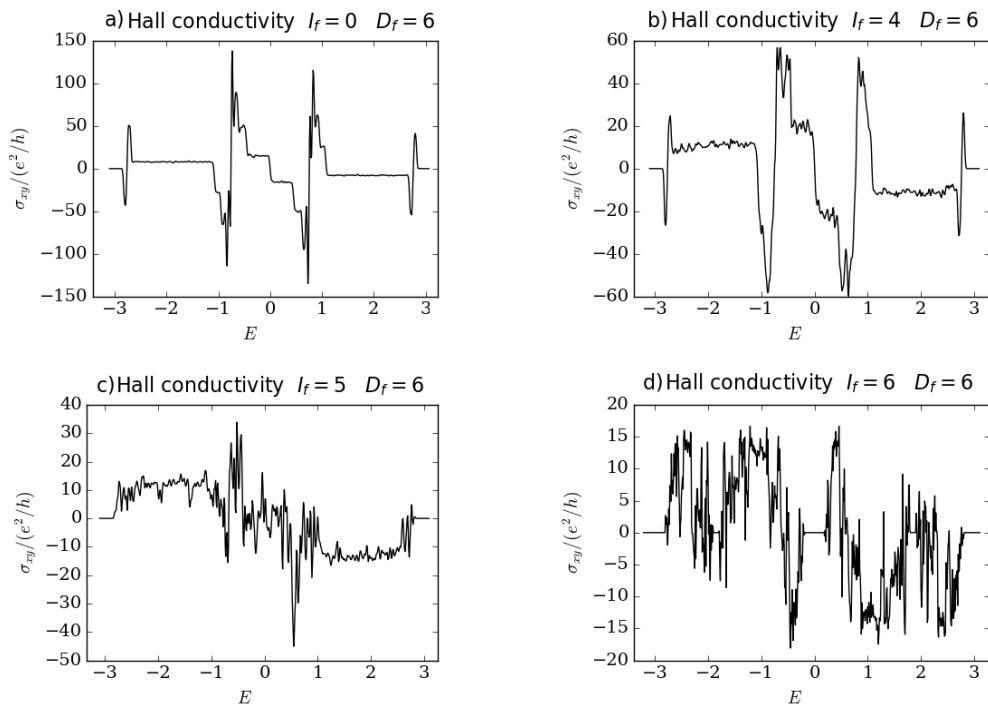


FIG. 4. The Hall conductivity for different iterations of Sierpinski carpet in a square of the size $3^{D_f} \times 3^{D_f}$ and $D_f = 6$ ($\Phi/\Phi_0 = 0.25$): a) is $I_f = 0$ iteration, b) is $I_f = 4$ iterations, c) is $I_f = 5$ iterations, d) is $I_f = 6$ iterations. As in the Fig. 2, the differences between a) and b) are small, only small fluctuations are added in b). Picture c) demonstrates transition to another phase, picture d) is very different from previous cases.

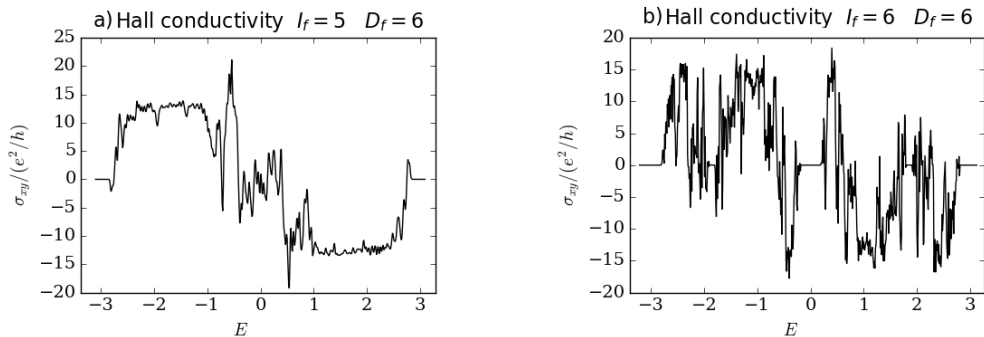


FIG. 5. The Hall conductivity for Sierpinski carpet with additional disorder in a square of the size $3^{D_f} \times 3^{D_f}$ and $D_f = 6$ ($\Phi/\Phi_0 = 0.25$): a) is $I_f = 5$ iteration, b) is $I_f = 6$ iterations. Approximately 20% sites are deleted. There are no visible differences from the Fig. 4

manifestation of full scaling symmetry of a fractal.

We see that for energies $E = 1.33$ and $E = 2.59$, which is in the region of almost quantized and quantized Chern number, edge states remain to be edge states. However, some part of plateaus of previous iterations with edge states become a bulk state. We also see that some bulk state in different iteration have similar localization properties. Accordingly, we can assume that there are states with different effective scale. Some of states feel only rough structure of a sample, some states feel smaller

holes.

We made calculation for various energies and they follow the described pattern. We see that quasi-eigenstates corresponding to the quantized Hall conductivity are localized along edges for iterations less than $I_f = 4$ (with maximum possible number of iterations equal to $D_f = 5$). It is also worth to notice that all edges, namely, the edge of the sample and the edges of the holes can make contribution to quasi-eigenstates. For most of quasi-eigenstates which have been calculated for various energies in the

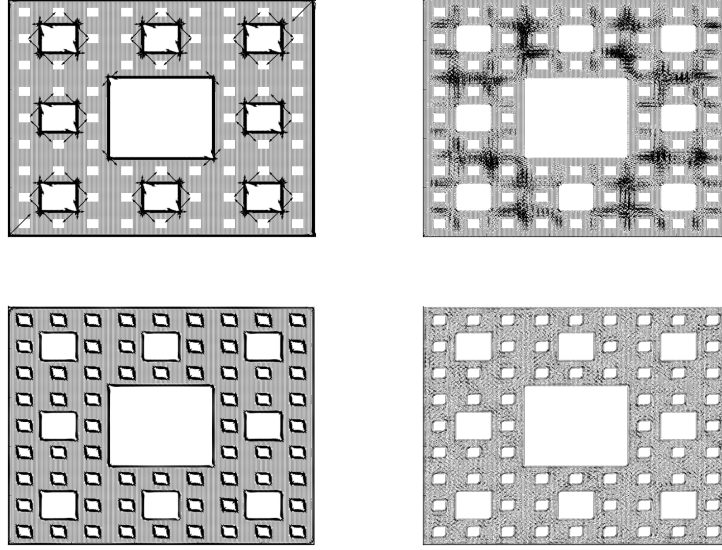


FIG. 6. Quasi-eigenstates for Sierpinski carpet with size $3^{D_f} \times 3^{D_f}$ with $D_f = 5$ and $I_f = 3$ iterations. Examples of edge states for energies $E = 1.51$ and $E = 2.59$ are on the left, examples of bulk states for energies $E = 1.09$ and $E = 2.83$ are on the right.

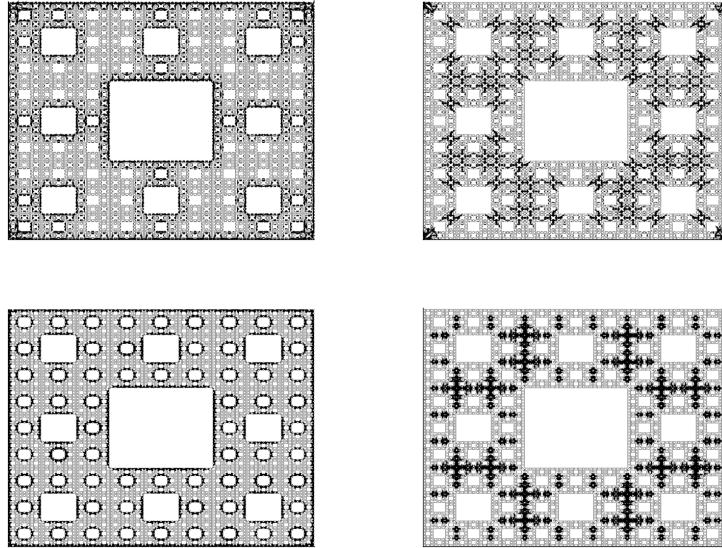


FIG. 7. Quasi-eigenstates for Sierpinski carpet with size $3^{D_f} \times 3^{D_f}$ with $D_f = 5$ and $I_f = 3$ iterations. Examples of edge states for energies $E = 1.33$ and $E = 2.59$ are on the lefts, examples of bulk states for energies $E = 1.57$ and $E = 2.83$ are on the right.

case of $I_f = 5$ and $D_f = 5$, there were no obvious domination of edge states.

We observe that the same transition, which already was observed in DoS and Hall conductivity, manifests in quasi-eigenstates, when the number iterations is one less than the possible number of iterations. In the case of bulk states, it manifests as more symmetric picture of current.

In the case of edge states, it manifests as more complex localization along edges, so that some edge states become localized along smaller holes, which are close to an edge.

SUMMARY

We see that with increasing depth of a fractal the quantization of Hall conductivity disappears. However, there is some reminiscence of topological nature of quantization, namely some plateaus remain. We also see that for Sierpinski carpet the relation between topological invariants such as Chern numbers and Hall conductivity does not work, contrary to the case of integer dimensions. The calculated conductivity is not proportional to Chern number, but fits similar pattern. One can speculate about possible reasons of it.

At first, the formula, which calculates Chern number through projectors, was proven to be properly defined only for systems with translational invariance [39]. Even if the formula works for fractals, it may be that one needs to calculate Hall conductivity and Chern numbers in thermodynamic limit. Another reason can be connected with difficulties with defining edge and bulk state. Some of the edge states are localized along inner holes. Particularly these states become closer to a bulk states in a full depth of fractal, so we cannot say is it localization along edges or localization on a small inhomogeneities. Edge states along big holes become also localized not only along edges, but also along small holes around an edge. These possible effects require future investigations.

We considered different iterations I_f of Sierpinski carpet on a fixed rectangular sample with size $3^{D_f} \times 3^{D_f}$. We observed that there is a transition between two different regimes, which occurs when $I_f = D_f - 1$. This transition can be seen in density of states, Hall conductivity and quasi-eigenstates. In the case of quasi-eigenstates, the edge states mostly become bulk states with increasing the iterations of Sierpinski carpet. This result can be explained due to effective dimension. If number of holes is finite, then the effective dimension of a sample is integer, not fractional. The transition occurs when holes in a sample are dense enough and effective dimension of a sample becomes non-integer.

The edge states can be localized along the borders of all holes of various scales, not only the edge of the sample. There is no big difference in amplitude for different holes. Edge states still can be seen for a full fractal, however, they change their character of localization. Additional holes along edges increase effective localization width. Therefore, one can speculate that if a state is localized along small holes and these holes are dense enough, there could be a transition from edge state to a bulk state.

When this work was finished the preprint [40] arises which treats a similar problem but in a technically different way (it is based on the use of Landauer formula rather than Kubo-Bastin formula and does not include an analysis of edge states). Qualitatively, the corresponding part of our conclusions is similar to the conclusions of that paper.

ACKNOWLEDGEMENTS

This work was supported by the National Science Foundation of China under Grant No. 11774269 and by the Dutch Science Foundation NWO/FOM under Grant No. 16PR1024 (S.Y.), and by the by the JTC-FLAGERA Project GRANSPOORT (M.I.K.). Support by the Netherlands National Computing Facilities foundation (NCF), with funding from the Netherlands Organisation for Scientific Research (NWO), is gratefully acknowledged.

* A.Iliasov@science.ru.nl

† s.yuan@whu.edu.cn

- [1] S. Havlin and D. Ben-Avraham, *Diffusion in disordered media*, Advances in Physics 36, 695 (1987).
- [2] L. Pietronero and E. Tosatti (Editors), *Fractals in physics*. (Elsevier, Amsterdam, 1986).
- [3] J. Feder, *Fractals* (Plenum Press, New York, 1988).
- [4] E. Domany, S. Alexander, D. Bensimon, and L. Kadanoff, *Solutions to the Schrödinger equation on some fractal lattices*, Phys. Rev. B 28, 3110 (1983).
- [5] M. Polini, F. Guinea, M. Lewenstein, H. C. Manoharan, and V. Pellegrini, *Artificial honeycomb lattices for electrons, atoms and photons*, Nature Nanotechnology 8, 625 (2013).
- [6] M. Gibertini, A. Singha, V. Pellegrini, M. Polini, G. Vignale, A. Pinczuk, L. N. Pfeiffer, and K. W. West, *Engineering artificial graphene in a two-dimensional electron gas*, Phys. Rev. B 79, 241406 (2009).
- [7] J. Shang, Y. Wang, M. Chen, J. Dai, X. Zhou, J. Kuttner, G. Hilt, X. Shao, J. M. Gottfried, and K. Wu, *Assembling molecular Sierpinski triangle fractals*, Nature Chemistry 7, 389 (2015).
- [8] S. N. Kempkes, M. R. Slot, S. E. Freeney, S. J. M. Zevenhuizen, D. Vanmaekelbergh, I. Swart, and C. Morais Smith, *Design and characterization of electrons in a fractal geometry*, Nature Physics 15, 127 (2018)
- [9] E. van Veen, S. Yuan, M. I. Katsnelson, M. Polini, and A. Tomadin, *Quantum transport in Sierpinski carpets*, Phys. Rev. B 93, 115428 (2016).
- [10] E. van Veen, A. Tomadin, M. Polini, M. I. Katsnelson, and S. Yuan, *Optical conductivity of a quantum electron gas in a Sierpinski carpet*, Phys. Rev. B 96, 235438 (2017).
- [11] Z.-G. Song, Y.-Y. Zhang, and S.-S. Li, *The topological insulator in a fractal space*, Appl. Phys. Lett. 104, 233106 (2014).
- [12] T. Westerhout, E. van Veen, M. I. Katsnelson, and S. Yuan, *Plasmon confinement in fractal quantum systems*, Phys. Rev. B 97, 205434 (2018).
- [13] D. Sticlet and A. Akhmerov, *Attractive critical point from weak antilocalization on fractals*, Phys. Rev. B 94, 161115 (2016)
- [14] A. Kosior and K. Sacha, *Localization in random fractal lattices*, Phys. Rev. B 95, 104206 (2017).
- [15] M. Brzezinska, A. M. Cook, and T. Neupert, *Topology in the Sierpinski-Hofstadter problem* Phys. Rev. B 98, 205116 (2018)

- [16] A. Agarwala, S. Pai, and V. B. Shenoy, *Fractalized Metals* ArXiv e-prints (2018), arXiv:1803.01404 [cond-mat.dis-nn].
- [17] A. K. Golmankhaneh, *Statistical Mechanics Involving Fractal Temperature* Fractal Fract. 3(2), 20 (2019)
- [18] I. Akal, *Entanglement entropy on finitely ramified graphs* Phys. Rev. D 98, 106003 (2018)
- [19] B. Pal and K. Saha, *Flat bands in fractal-like geometry* Phys. Rev. B 97, 195101 (2018)
- [20] A. Nandy and A. Chakrabarti, *Engineering slow light and mode crossover in a fractal-kagome waveguide network* Phys. Rev. A 93, 013807 (2016)
- [21] D. J. Thouless, M. Kohmoto, M. P. Nightingale, and M. den Nijs, *Quantized Hall conductance in a two-dimensional periodic potential*, Phys. Rev. Lett. 49, 405 (1982)
- [22] D.-C. Tran, A. Dauphin, N. Goldman, and P. Gaspard, *Topological Hofstadter insulators in a two-dimensional quasicrystal*, Phys. Rev. B 91, 085125 (2015)
- [23] Y. E. Kraus and O. Zilberberg, *Topological Equivalence between the Fibonacci Quasicrystal and the Harper Model*, Phys. Rev. B 91, 085125 (2012)
- [24] Bellissard J. *Gap Labelling Theorems for Schrödinger Operators*. In: M. Waldschmidt, P. Moussa, JM. Luck, C. Itzykson (eds) From Number Theory to Physics. Springer, Berlin, Heidelberg (1992)
- [25] E. Prodan *Disordered topological insulators: a noncommutative geometry perspective*, J. Phys. A: Math. Theor. 44, 239601 (2011)
- [26] J. Bellissard, A. van Elst, and H. SchulzBaldes *The noncommutative geometry of the quantum Hall effect*, J. Math. Phys. 35, 5373 (1994)
- [27] G. B. Halasz, T. H. Hsieh, and L. Balents, *Fracton topological phases from strongly coupled spin chains*, Phys. Rev. Lett. 109, 116404 (2017)
- [28] T. Devakul, Y. You, F. J. Burnell, S. L. Sondhi, *Fractal symmetric phases of matter* SciPost Phys. 6, 007 (2019)
- [29] B. I. Halperin, *Quantized Hall conductance, current-carrying edge states, and the existence of extended states in a two-dimensional disordered potential* Phys. Rev. B 25, 2185 (1982)
- [30] Y. Hatsugai, *Chern number and edge states in the integer quantum Hall effect* Phys. Rev. Lett. 71, 3697 (1993)
- [31] R. S. K. Mong and V. Shivamoggi, *Edge states and the bulk-boundary correspondence in Dirac Hamiltonians* Phys. Rev. B 83, 125109 (2011)
- [32] A. Hams and H. De Raedt, *Fast algorithm for finding the eigenvalue distribution of very large matrices*, Phys. Rev. E 62, 4365 (2000)
- [33] S. Yuan, H. De Raedt, and M. I. Katsnelson, *Modeling electronic structure and transport properties of graphene with resonant scattering centers* Phys. Rev. B 82, 115448 (2010)
- [34] J. H. Garca, L. Covaci, and T. G. Rappoport, *Real-space calculation of the conductivity tensor for disordered topological matter* Phys. Rev. Lett. 114, 116602 (2015)
- [35] S. Yuan, E. van Veen, and M. Katsnelson, R. Roldan, *Quantum Hall effect and semiconductor-to-semimetal transition in biased black phosphorus*, Phys. Rev. B 93, 245433 (2016)
- [36] D. R. Hofstadter, *Energy levels and wave functions of Bloch electrons in rational and irrational magnetic fields* Phys. Rev. B 14, 2239 (1976)
- [37] R. E. Prange and S. M. Girvin (Editors), *The quantum Hall effect* (Springer, Berlin, 1987).
- [38] K. Hornberger, U. Smilansky, *Magnetic edge states* Physics Reports 367, 249 (2002)
- [39] A. Kitaev, *Anyons in an exactly solved model and beyond* Annals of Physics 321, 2111 (2006)
- [40] M. Fremling, M. van Hooft, C. Morais Smith, and L. Fritz, *A Chern insulator in $\ln(8)/\ln(3)$ dimensions* arXiv:1906.07387